Proceedings of the INMM & ESARDA Joint Virtual Annual Meeting
August 23-26 & August 30-September 1, 2021

Benchmarking Monte Carlo Simulations in the context of nuclear disarmament verification via Monte Carlo simulations with GEANT4

Manuel Kreutle[1], Alessandro Borella[2], Riccardo Rossa[2], Celine Scholten[1], Gerald Kirchner[1], Claas van der Meer[2]

[1]: Carl-Friedrich von Weizsäcker-Center for Science and Peace Research, Universität Hamburg, Hamburg, Germany.

[2]: Belgian Nuclear Research Centre SCK CEN, Mol, Belgium.

Abstract

As part of the work of the International Partnership for Nuclear Disarmament Verification (IPNDV), an international exercise was held at the site of the Belgian Nuclear Research Centre SCK CEN in Mol, Belgium. In addition to the measurements, Monte Carlo simulations were performed to simulate the neutron signatures of the different set-ups. In this paper simulation results are presented for the effective neutron multiplication factor k_{eff}, neutron flux densities, (α,n) spectra and spatial distributions of neutron interactions processes obtained with GEANT4. We compare GEANT4's k_{eff} results with MCNP and KENO simulations and can demonstrate its good performance. We further observe a good agreement in the comparison of flux densities for epithermal and fast neutrons calculated by GEANT4 and KENO. The only significant deviations were observed for thermal neutrons after interacting with bound hydrogen atoms in Polyethylene. Our results contribute to the validation of GEANT4 neutron physics in fissile material systems as a nuclear disarmament verification environment.

1 Introduction

Between 9th and 26th of September 2019 as part of the work of the International Partnership for Nuclear Disarmament Verification (IPNDV), a measurement campaign was conducted at the Belgian Nuclear Research Centre SCK CEN in Mol, Belgium. Its objective was to test various detectors for their potential use for nuclear disarmament verification. Non-destructive passive measurement techniques were applied to close-to-weapons grade plutonium present in form of unirradiated plutonium-uranium MOX fuel elements.

Monte Carlo simulations were performed with GEANT4, KENO and MCNP analyzing the neutron and gamma characteristics of the nuclear material with various shielding conditions. Special focus was put on the GEANT4 simulation software, which was developed in 1999 at

CERN [1]. Initially intended for a use in high energy particle physics, it has transformed into a widespread tool for particle transport calculations with applications in medical physics [2], space engineering [3], nuclear physics [4] and other fields. In nuclear physics applications it has already been validated in a few occasions but a wider basis is still desired [5]. The following paper investigates the performance of GEANT4 and compares its results to KENO and MCNP results to contribute to the validation efforts.

2 Methods

2.1 Simulated set-up

The IPNDV Technology Demonstration performed at SCK CEN in Mol, Belgium provided various assemblies: Three types of fuel rods in different numbers and with various shielding materials (see *Borella et al., "A Measurement Campaign In Support Of Technologies For Disarmament Verification", this conference, [6]*).
We simulated MOX fuel with a ^{239}Pu content of 62%$_{wt}$ within a plutonium content of 12.6%$_{wt}$, with 1, 19 and 61 fuel rods of 100 cm length. They are referred to as 62-1, 62-19 and 62-61. Another simulated configuration is called 79-19 and has a ^{239}Pu content of 79%$_{wt}$ within plutonium with 19 fuel rods of 50 cm length. The 96-19 configuration has also 19 fuel rods of 50 cm length but comes only with a central section of 96%$_{wt}$ ^{239}Pu MOX and other MOX types on the top and the bottom (for a more detailed description of the axialy heterogeneous structure see [6]). Simulated shielding conditions are the bare assemblies and assemblies with a 5 cm layer of Polyethylene (PE), a 0.11 cm layer of cadmium (Cd) or the combination of PE with 1 cm of lead (Pb).
In a later part of the analysis, a configuration which as such was not present in Mol was simulated: a 61 rods assembly of the 96%$_{wt}$ MOX fuel. In this analysis additionally two different types of shielding were simulated which were not available during the exercise: Pb+PE and Cd+PE. Here the metals (Pb: 1cm; Cd: 0.11cm) were placed before adding 5cm of PE.

All simulations were executed including locking plate and aluminum palette. Single screws and lids were omitted.

2.2 Simulation codes

Neutronic characteristics of the simulated experimental set-up was simulated with the Monte Carlo codes GEANT4 version 10.05.1, MCNP-6 [7], and KENO-IV [8].
Due to the presence of fissile material in oxide form, along with the spontaneous fission neutrons (mainly originating from ^{240}Pu) ^{17}O(α,n)^{20}Ne and ^{18}O(α,n)^{21}Ne reactions take a significant role. As the standard GEANT4 version does not include (α,n) reactions it had to be extended by the SaG4n tool [9]. We compare SaG4n's results with the results generated by ORIGEN [8].

2.3 Cross section libraries

GEANT4 simulations in this paper mainly rely on the ENDF/B-VIII.0 cross section library. For thermal neutron scattering ENDF-B/VI.2 cross sections were used. Fission processes were

simulated with an implementation of the LLNL fission model [10]. The used MCNP version relies on the ENDF-B/VII.1 cross section library, KENO on ENDF-B/VII.0 (if not stated otherwise).

SaG4n used cross sections from JENDL/AN-2005 [11] and TENDL-2017 [12] to calculate the neutron production from (α,n) reactions. α emission data was taken from the Bureau international des poids et mesures's Table of Radionuclides Vol.5 [13].

2.4 Data generation

GEANT4 - in contrast to codes like MCNP and KENO - does not directly provide the effective neutron mutliplication factor k_{eff} and therefore had to be extended. We used an approach that counts neutrons originating from fission if their parents have already done so. For each generation GEANT4's track IDs are stored in a vector. If a neutron's parent ID can be found in an earlier generation's vector it is assigned to the next generation. From that, k_{eff} is calculated. Track IDs of neutrons scattering inelastically in between have to be replaced in their corresponding vectors.

For our analysis we define *flux density* as $\Phi = (\Sigma_{k=1}^{K} l_k)/V$ with K being the number of particles crossing a volume V, each with a track length of l_k. Flux densities and corresponding energy distributions were calculated for neutrons leaving the set-up and crossing a predefined volume - further referred to as *reference volume*. It measures 10 cm x 10 cm x 0.5 cm and was placed in parallel to the fuel element channel in a distance of 6 cm to the surface. The center of the reference volume was aligned with the center of the fuel rods. We also use the underlying information on the number of neutrons crossing the reference volume and their mean track length.

In contrast to KENO and MCNP, GEANT4 allows to extract the locations of simulated reactions and thus obtaining a spatial distributions of elastic scattering, neutron capture or neutron-induced fission within the IPNDV exercise configurations. Results are displayed in 2-dimensional histograms ("heat maps") and will be given below.

3 Results and discussion

3.1 Comparison of k_{eff}

As seen in Tables 1 and 2, the k_{eff} results of GEANT4 agrees well with KENO and MCNP. The only exception is a 6% deviation of GEANT4 with respect to KENO and MCNP for the cases of the PE+Pb shielded 79-19 configuration. This overall indicates a good performance of GEANT4.

Table 1: Simulated k_{eff} for the configuration with 79%$_{wt}$ ^{239}Pu content, 19 fuel rods and various shielding.

Code	Nuclear data library	$k_{eff} \pm \sigma$ bare	Cd	PE + Pb
MCNP	ENDF/B-VII.1	0.05135 ± 0.00002	0.05150 ± 0.00002	0.17020 ± 0.00013
KENO-VI	ENDF/B-VII.0	0.05284 ± 0.00004	0.05299 ± 0.00004	0.16749 ± 0.00011
	ENDF/B-VII.1	0.05292 ± 0.00003	0.05302 ± 0.00003	0.16687 ± 0.00012
Geant4	ENDF/B-VIII.0	0.05211 ± 0.00004	0.05143 ± 0.00003	0.18023 ± 0.00007

Table 2: Simulated k_{eff} for the configuration with 62%$_{wt}$ ^{239}Pu content, 1/19/61 fuel rod(s) and with PE shielding.

Code	Nuclear data library	$k_{eff} \pm \sigma$ 1 rod	19 rods	61 rods
MCNP	ENDF/B-VII.1	0.04343 ± 0.00007	0.19451 ± 0.00015	0.30817 ± 0.00017
KENO-VI	ENDF/B-VII.0	0.04388 ± 0.00013	0.18924 ± 0.00029	0.29529 ± 0.00031
	ENDF/B-VII.1	0.04355 ± 0.00014	0.18718 ± 0.00030	0.29289 ± 0.00038
Geant4	ENDF/B-VIII.0	0.04146 ± 0.00011	0.18859 ± 0.00011	0.30323 ± 0.00012

3.2 Comparison of flux densities and spectra

As k_{eff} is a bulk value, we extent our analysis by a comparison of neutron flux densities and their energy distributions simulated with GEANT4 and KENO.

The reference volume neutron flux densities were simulated for the 79-19 configuration. Results are given in Table 3. We observe a good agreement between the codes with GEANT4 deviating $< 8\%$ for the bare and $< 4\%$ for the Cd-shielded 79-19 configuration with respect to the KENO results. Results for the PE+Pb shielded configuration deviate stronger. Changing from Cd to PE+Pb, the total flux density - in contrast to a decrease for KENO - increases for GEANT4 and exceeds the KENO value by ∼20%. A closer look revealed that for a change from 79-19 Cd to 79-19 PE+Pb the number of neutrons entering the volume decreased also for GEANT4 (Cd: 24.7 $\text{cm}^{-2}\text{s}^{-1}$; PE+Pb: 21.0 $\text{cm}^{-2}\text{s}^{-1}$) by 15%. This is very similar to KENO. It is the increase in the neutrons' mean track length within the reference volume which for GEANT4 led to an increase in the flux density.

Flux densities within the 252-group energy intervals and corresponding relative deviations between KENO and GEANT4 with respect to KENO can be found in Figure 1. For the Cd-shielded case, deviations within the energy intervals individually scatter between -40% and +20% but in the mean result in a deviation of only -8% (Figure 1: Bottom left). For the PE+Pb-shielded configuration we see a fairly well agreement between the codes for fast neutrons ($E \geq 10^2$ eV) with a mean relative deviation of $\sim 6\%$. The epithermal range (10^{-1} eV$< E < 10^2$ eV) with multiple absorption resonances is not covered very well, as a mean deviation of ∼30% shows. For the thermal energy range ($\leq 10^{-1}$ eV) a big neutron surplus is observed with GEANT4 deviating by +87% with respect to KENO. This is difficult to assess due to the still incomplete crosssectional representation of thermal neutron interactions with

PE-bound hydrogen atoms on the side of KENO. More validation is needed here.

Table 3: Comparison of calculated flux densities through the reference volume for the configuration with 79%$_{wt}$ ^{239}Pu content, 19 fuel rods and with different shielding (given in *neutrons* $cm^{-2}s^{-1}$).

Shielding	Bare	Cd	PE+Pb
KENO	34.2 ± 0.1	34.0 ± 0.1	28.9 ± 0.1
GEANT4	31.6 ± 0.4	32.9 ± 0.4	34.4 ± 0.4

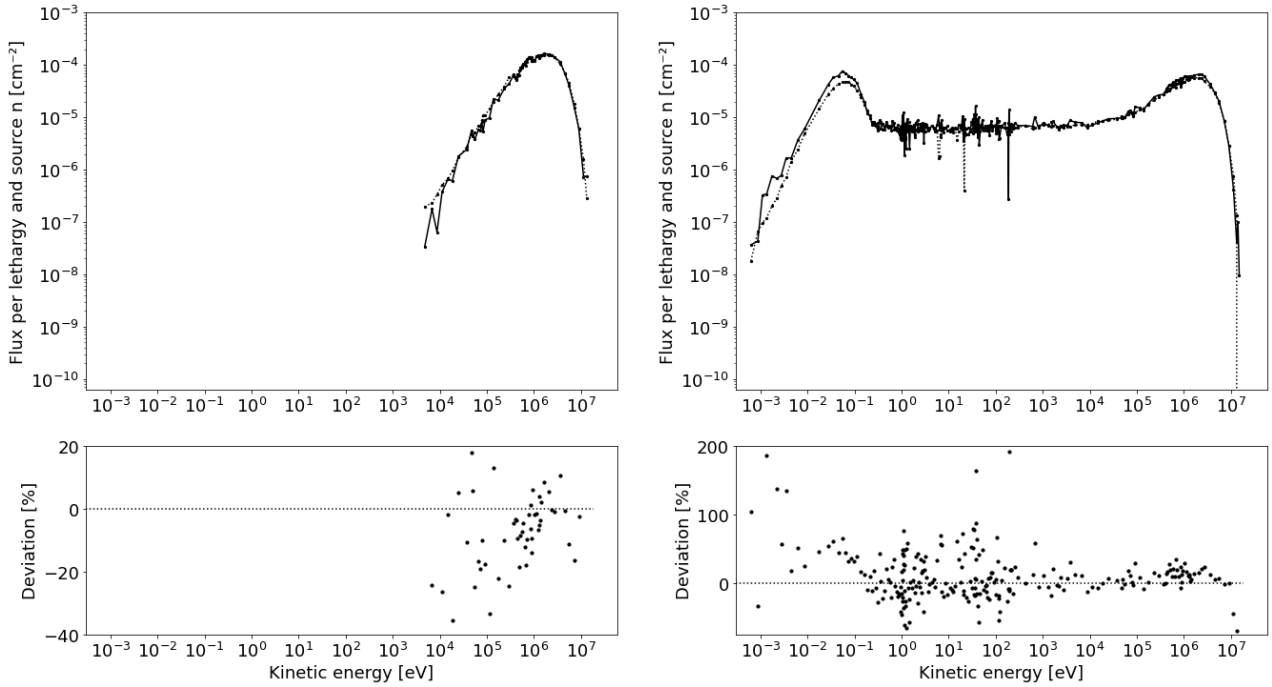

Figure 1: **Left:** Cdshielding; **Right:** PE+Pb shielding.
Top: Comparison of the flux per lethargy and source neutron within 252 energy groups for neutrons originating from the Cd-shielded 79%$_{wt}$, 19 fuel rods configuration and entering the reference volume (Continuous: GEANT4; dashed: KENO).
Bottom: Relative deviation (GEANT4-KENO)/KENO.

3.3 Comparison of (α, n) codes

Energy spectra for neutrons originating from (α,n) reactions were calculated with SaG4n and ORIGEN and are shown in Figures 2 and 3. Due to SaG4n's particlewise output, small emission probabilities are directly linked to the number of simulated events and are therefore not covered as good as they are by ORIGEN. Around energies of order 1 MeV the spectrum generated with ORIGEN deviates from SaG4n in terms of much wider energy intervals. When using both spectra as (α,n) input data for GEANT4 simulations these deviations were still observable in

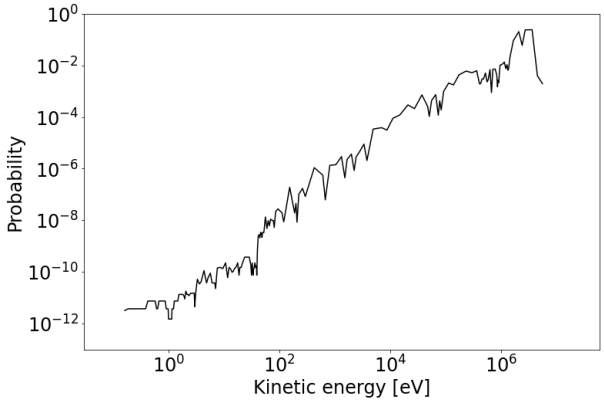

Figure 2: (α,n) energy spectrum generated with ORIGEN.

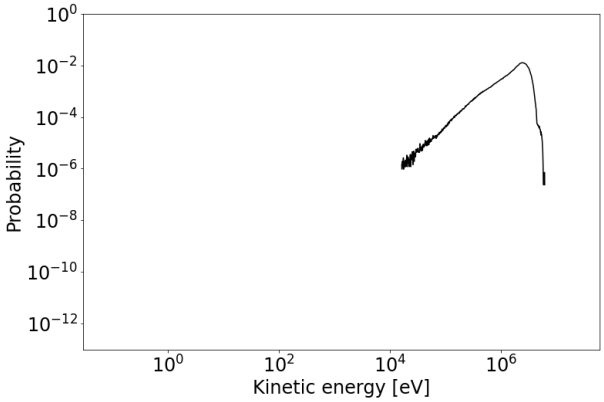

Figure 3: (α,n) energy spectrum generated with SaG4n.

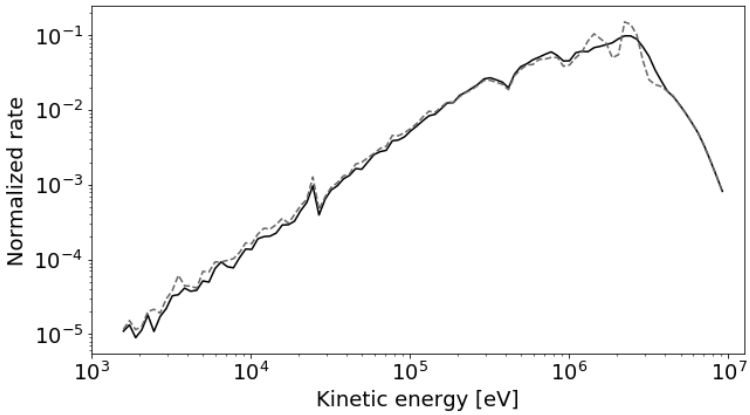

Figure 4: Comparison of normalized count rate (a.u.) of neutrons leaving the bare 62%$_{wt}$, 61 fuel rods configuration and entering the face of the reference volume obtained with GEANT4 (*Continuous: SaG4n (α,n) input spectrum; dashed: ORIGEN (α,n) input spectrum.*

form of strong peaks in a spectrum taken at the reference area for the bare 62%$_{wt}$, 61 fuel rods configuration (see Figure 4). Both recorded spectra in general do not deviate more than 10% with respect to the SaG4n spectrum except for the mentioned region where a deviation of $20-30\%$ is observed. On the other hand total neutron flux densities at the reference volume ($\Phi_{\mathrm{SaG4n}} = 333 \pm 1\ cm^{-2}s^{-1}$ and $\Phi_{\mathrm{ORIGEN}} = 334 \pm 1\ cm^{-2}s^{-1}$) and neutron multiplication behavior ($\mathrm{k_{eff}} = 0.3377 \pm 0.0004$ for both cases) do not deviate for the two input spectra. We therefore conclude that SaG4n and ORIGEN agree well for the simulated set-up.

3.4 Spatial distribution of neutron interaction processes

Based on the GEANT4 feature to allow for extraction of locations of simulated reactions, Figures 5 a), d) and 7 a), d) show that spatial distributions for the bare and the Cd-shielded configurations vary insignificantly for fission and elastic scattering with most reactions taking place in the center. Slightly more capture reactions are seen in the shielding plate when using

the neutron absorber Cd, as seen in Figure 6 a), d). The combinations of metal and PE however affect the distributions more strongly (see Figure 5 b). Pb+PE shiedling causes more fission reactions which mostly occur at the edge ot the hexagonal assembly due to the reentry of moderated neutrons with a higher fission cross section. A Cd-plate instead of Pb decreases this gradient due to its' significant absorption cross section for thermal neutrons, although an increase in the number of fission reactions is still apparent. The moderation effect can be observed in Figures 7 b), c) and 8 b), c) where most elastic scattering reactions are located within the PE layer. The structure of the axially heterogeneous 96-61 assembly is reflected by the different neutron scattering rates of the various fuel segments (see Figure 8).
The distributions underline the significant influence of shielding materials on fissile material behavior.

4 Conclusions

The IPNDV experiments covers the full neutron energy range from thermal via epithermal to fast neutron spectra with close-to-weapons grade Pu and shielding materials to mimic warhead and container components. Only the oxide form of fissile material and consequent (α,n) emissions are not be expected for nuclear warheads but produce an elevated neutron background. Various of these experimental configurations were simulated with GEANT4, KENO and MCNP. GEANT4's results for the neutron multiplication factor k_{eff} are very well in line with MCNP and KENO. Neutron Flux densities obtained with GEANT4 and KENO agree for epithermal and fast neutron energies as observed in the bare and Cd-shielded configurations but deviate significantly for thermal neutron energies resulting from PE+Pb shielding. Small deviations were observed for (α,n) simulations with SaG4n (additional Geant4 tool) and ORIGIN but without significant effects on GEANT4 simulations and results for k_{eff} and flux densities. The analysis of the spatial distribution of different neutron interaction processes - a unique feature of GEANT4 - underlines the significant influence of shielding materials on fissile material behavior under nuclear disarmament verification conditions.
The presented data contributes to the validation of GEANT4 neutron physics in fissile material systems and in a nuclear disarmament verification environment.

Acknowledgments

One of the authors (M.K.) would like to thank SCK CEN and its members for the opportunity to take part in the measurement campaign and their hospitality.

References

[1] Agostinelli, S. et al. (2003). "GEANT4 — a simulation toolkit". In: Nuclear Instruments and Methods in Physics Research A 506, pp. 250–303.

[2] Lechner, A. et al. (2010). "Validation of recent Geant4 physics models for application in carbon ion therapy", In: NIM B 268, pp. 2343-2354.

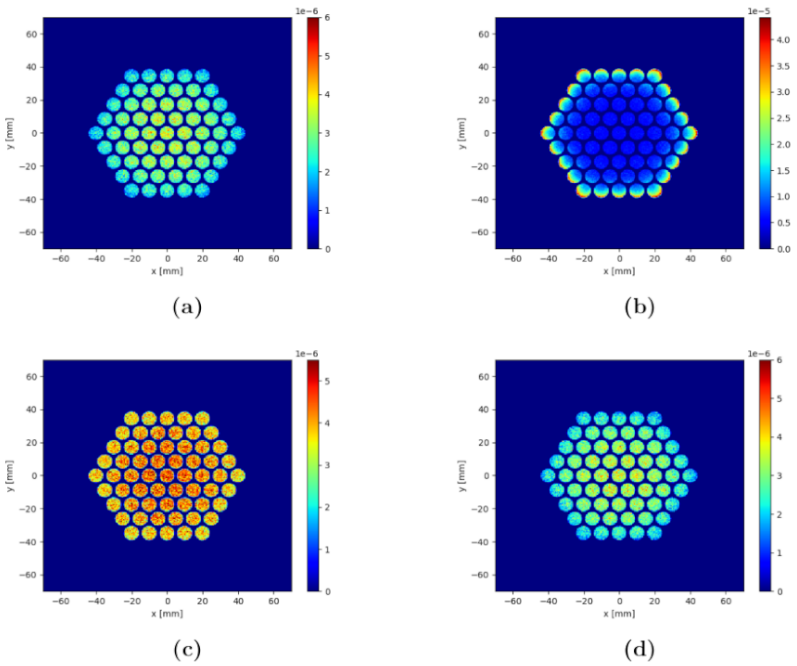

Figure 5: Spatial distirbution of fission reactions per source neutron in 62%$_{wt}$, 61 fuel rods configuration with a) no shielding, b) Pb+PE, c) Cd+PE, and d) Cd shielding. (Resolution: 0.5cm x 0.5cm within the whole fuel rod length).

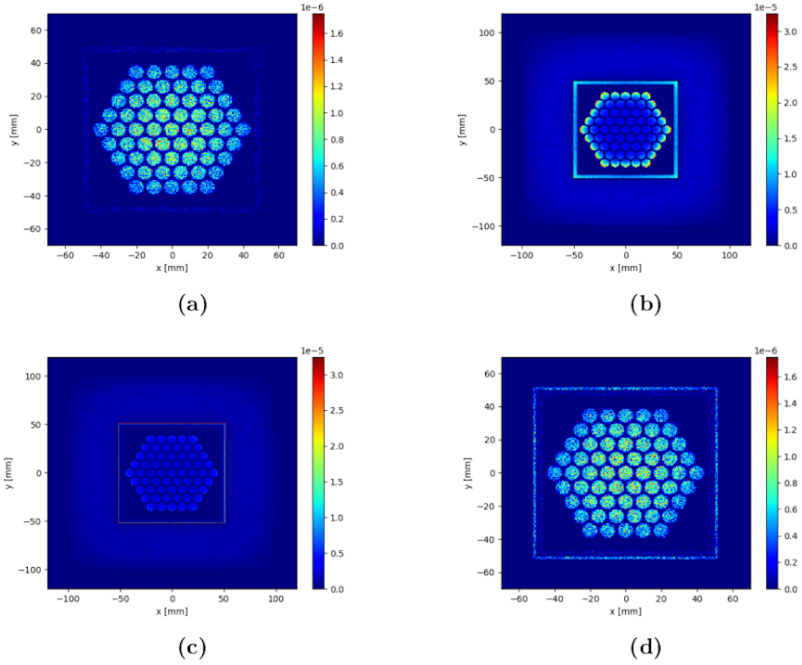

Figure 6: Spatial distirbution of neutron capture reactions per source neutron in 62%$_{wt}$, 61 fuel rods configuration with a) no shielding, b) Pb+PE, c) Cd+PE, and d) Cd shielding. (Resolution: 0.5cm x 0.5cm within the whole fuel rod length).

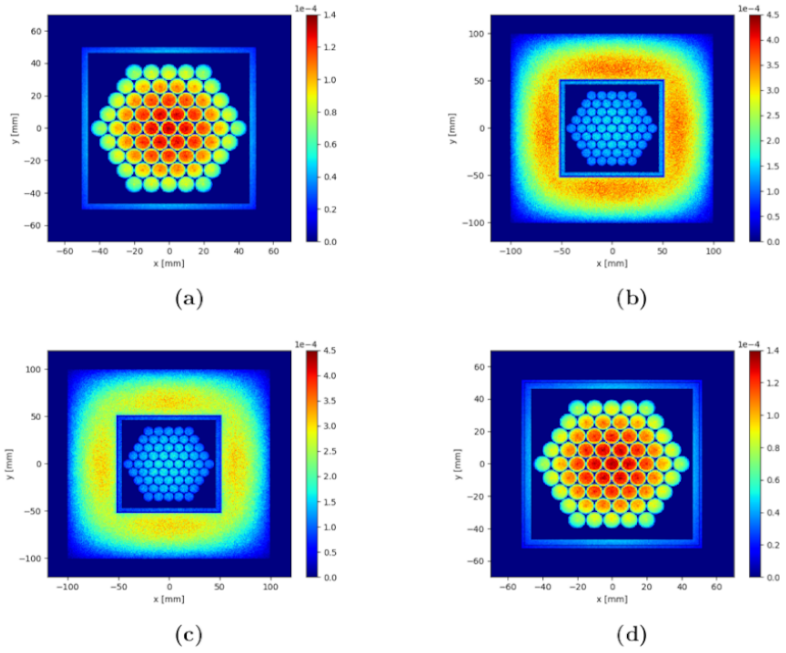

Figure 7: Spatial distirbution of elastic scattering reactions per source neutron in 62%$_{wt}$, 61 fuel rods configuration with a) no shielding, b) Pb+PE, c) Cd+PE, and d) Cd shielding. (Resolution: 0.5cm x 0.5cm within the whole fuel rod length).

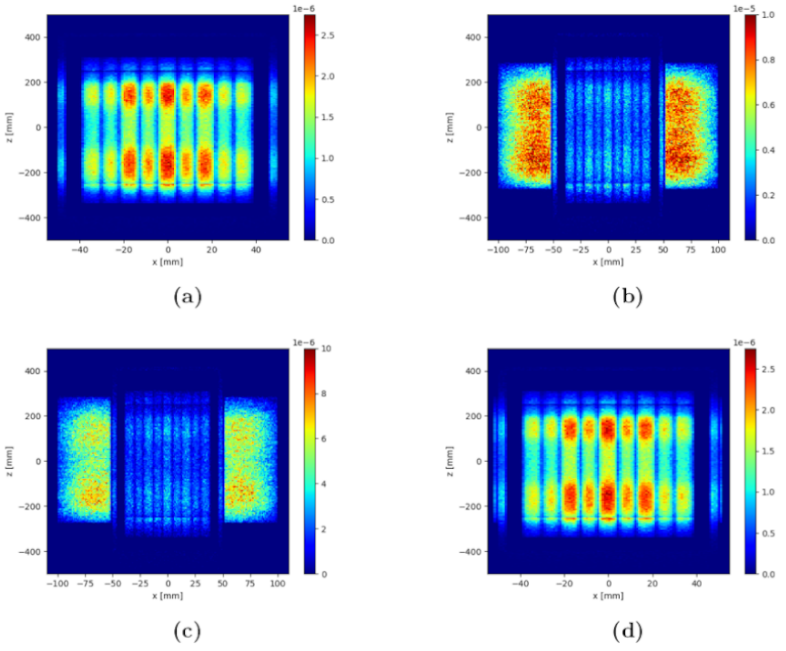

Figure 8: Spatial distirbution of elastic scattering reactions per source neutron in 79%$_{wt}$, 61 fuel rods configuration* with a) no shielding, b) Pb+PE, c) Cd+PE, and d) Cd shielding. (Resolution: 1cm x 4cm; in a centered slice of 0.8cm thickness).
*: simulated only, not present during IPNDV exercise.

[3] Ivantchenko A. et al. (2012). "Geant4 hadronic physics for space radiation environment". In: International Journal of Radiation Biology 88(1–2), pp. 171–17.

[4] Heikkinen A. et al. (2010). "A Geant4 physics list for spallation and related nuclear physics applications based on INCL and ABLA models". In: Phys.: Conf. Ser.219 032043.

[5] Mendoza, E. et al. (2014). "New Standard Evaluated Neutron Cross Section Libraries for the GEANT4 Code and First Verification". In: IEEE Transactions on Nuclear Sience 61.4, pp. 2357–2364.

[6] Borella et al. (2021). "A Measurement Campaign In Support Of Technologies For Disarmament Verification". In: Proceeding of INMM & ESARDA Joint Annual Meeting 2021 (this volume).

[7] Werner, C. J. et al. (2018). MCNP 6.2 Release Notes. Los Alamos National Laboratory. Los Alamos, New Mexico, USA.

[8] Rearden, B. T. and M. A. Jessee (2016). SCALE Code System. Oak Ridge National Laboratory. Oak Ridge, Tennessee, USA.

[9] Mendoza, E. et al. (2020). "Simulation of (a,xn) reactions with Geant4, User's Manual". Ministry of Science and Innovation, Nuclear Innovation Unit (CIEMAT), Madrid, Spain.

[10] Verbeke, J. M., C. Hagmann, and D. Wright (2014). "Simulation of Neutron and Gamma Ray Emission from Fission and Photofission". In: UCRL-TR-228518. Lawrence Livermore National Laboratory.

[11] Murata, T., H. Matsunobu, and K. Shibata (2006). "Evaluation of the (a,xn) Reaction Data for JENDL/AN-2005". In: JAEA-Research 52.

[12] Rochman, D. et al. (2016). "The TENDL library: hope, reality and future". In: Proceedings of the International Conference on Nuclear Data for Science and Technology, September 11-16, Bruges, Belgium: OECD Nuclear Energy Agency, pp. 97–102..

[13] Bé, M.-M. et al. (2010). Table of Radionuclides. Vol. 5. Monographie BIPM-5. Sèvres, France: Bureau International des Poids et Mesures.